Research Article

Resveratrol Derivative, Trans-3, 5, 4$'$-Trimethoxystilbene Sensitizes Osteosarcoma Cells to Apoptosis via ROS-Induced Caspases Activation

Yu Feng,[1,2] Jacob Clayton,[3] Wildman Yake,[3] Jinke Li,[3] Weijia Wang [ID],[4] Lauren Winne [ID],[3] and Ming Hong [ID][5,6]

[1]Department of Traumatology, General Hospital of Ningxia Medical University, 804 Shengli South Road, Yinchuan, Ningxia Hui Autonomous Region 750004, China

[2]Department of Orthopaedics and Traumatology, The University of Hong Kong, 21 Sassoon Road, Hong Kong SAR 999077, China

[3]Department of Pharmacology & Toxicology, University of Kansas, 126 Strong Hall, Lawrence, KS 66045, USA

[4]Zhongshan People's Hospital, 2 Sun Wen East Road, Zhongshan, Guangdong 528400, China

[5]Institute of Advanced Diagnostic and Clinical Medicine, Zhongshan People's Hospital, Guangzhou University & Zhongshan People's Hospital Joint Biomedical Institute, 2 Sun Wen East Road, Zhongshan, Guangdong 528400, China

[6]Dongguan & Guangzhou University of Chinese Medicine Cooperative Academy of Mathematical Engineering for Chinese Medicine, Building 16, Songke Garden, Songshan Lake Science and Technology Industrial Park, Dongguan 523000, China

Correspondence should be addressed to Weijia Wang; 530837226@qq.com, Lauren Winne; winnie_lsh@ku.edu, and Ming Hong; hongming530@126.com

Numerous studies have shown that resveratrol can induce apoptosis in cancer cells. Trans-3, 5, 4$'$-trimethoxystilbene (TMS), a novel derivative of resveratrol, is a more potent anticancer compound than resveratrol and can induce apoptosis in cancer cells. Herein, we examined the mechanisms involved in TMS-mediated sensitization of human osteosarcoma (143B) cells to TNF-related apoptosis-inducing ligand- (TRAIL-) induced apoptosis. Our results showed that cotreatment with TSM and TRAIL activated caspases and increased PARP-1 cleavage in 143B cells. Decreasing cellular ROS levels using NAC reversed TSM- and TRAIL-induced apoptosis in 143B cells. NAC abolished the upregulated expression of PUMA and p53 induced by treatment with TRAIL and TSM. Silencing the expression of p53 or PUMA using RNA interference attenuated TSM-mediated sensitization of 143B cells to TRAIL-induced apoptosis. Knockdown of Bax also reversed TSM-induced sensitization of 143B cell to TRAIL-mediated apoptotic cell death. These results indicate that cotreatment with TRAIL and TSM evaluated intracellular ROS level, promoted DNA damage, and activated the Bax/PUMA/p53 pathway, leading to activation of both mitochondrial and caspase-mediated apoptosis in 143B cells. Orthotopic implantation of 143B cells in mice also demonstrated that cotreatment with TRAIL and TSM reversed resistance to apoptosis in cells without obvious adverse effects in normal cells.

1. Introduction

Resveratrol, a natural polyphenolic compound that is abundant in blueberries, grapes, and peanuts, possesses numerous pharmacological activities. Previous studies have shown that resveratrol can induce apoptosis in various human tumor cells via ROS-dependent endoplasmic reticulum (ER) stress [1, 2]. Although resveratrol has shown remarkable anticancer effects in numerous preclinical studies, its poor pharmacokinetic parameters have restricted its clinical application. Adding methoxy or hydroxyl groups to the stilbene backbone of resveratrol generates modified resveratrol derivatives that possess improved bioavailability and stability, resulting in increased transport of these agents into cells [3]. Unlike

resveratrol, TMS can bind membrane proteins with high binding affinity. Furthermore, upon uptake, TMS can enter cells unaltered, which increases its stability within cells [4–6].

In recent decades, several studies have shown that TMS can exert antitumor effects in several malignant human tumors, including lung malignancies, cholangiocarcinoma, prostate adenocarcinoma, and osteosarcoma [7–9]. Annick et al. have demonstrated that TMS exhibits stronger anticancer activity than that of resveratrol and can induce apoptosis in malignant MCF-7 cells [10, 11]. Additionally, TMS can decrease cellular viability and induce apoptosis in prostate adenocarcinoma cells. This TMS-mediated inhibition of cellular viability can be enhanced by combining TMS with TRAIL, thereby activating the reactive oxygen species- (ROS-) induced caspase cascade [12]. Indeed, $20\,\mu$M TSM increases intracellular ROS levels and induces apoptosis by phosphorylating JNK, p38, and MAPK [13, 14]. Another study has shown that $10\,\mu$m TSM sensitizes osteosarcoma cells to apoptosis by activating Bax, p53, and caspase-3 [15]. Additionally, $10\,\mu$m TMS suppresses the proliferation of human hepatocellular carcinoma MHCC-97H cells by inducing PUMA-dependent cellular apoptosis in vitro and in vivo, suggesting that TMS may sensitize cancer cells to apoptosis [16]. Although TMS possesses reduced cytotoxicity compared with that of resveratrol, $10\,\mu$m TMS may show some cytotoxicity in normal cells and tissues [17]. Therefore, in our current study, we treated osteosarcoma cells with TRAIL and low-dose TMS ($2.5, 5\,\mu$m) to evaluate whether TMS could sensitize these cells to TRAIL-mediated apoptotic cell death.

ROS induce apoptosis by destroying the basic structure of DNA, which increases the expressions of PUMA and Bax [11, 12]. As a proapoptotic protein, Bax can promote cytochrome C release from the mitochondria and induces subsequent caspase cascade. Excessive levels of intracellular ROS and DNA damage may activate the expression of p53 and upregulate that of PUMA, subsequently inducing cellular apoptosis [13]. Previous studies have shown that TMS ($10\,\mu$m) may inhibit cancer progression by promoting PUMA-dependent apoptosis [9]. Hence, we hypothesized that in osteosarcoma cells, treatment with TMS likely triggers Bax/PUMA/P53 signaling that contributes to intrinsic apoptosis, while cotreatment with TRAIL and TMS likely induces extrinsic apoptosis. To test this hypothesis, we treated osteosarcoma cells with TRAIL and low-dose TMS to evaluate whether TMS could sensitize these cells to TRAIL-mediated apoptosis.

2. Materials and Methods

2.1. Cell Lines and Chemicals. Osteosarcoma cells 143B and Saos-2 were provided by Dr. Christopher Johnson (Medical center, University of Kansas); the MG-63 cells with specific genes knock-down were purchased form GeneTech corporation (San Francisco, CA, USA). Normal human osteoblast hFOB1.19 cells were provided by Dr. Ryan Taylor (Medical center, University of Kansas). hFOB1.19 cell was cultured in complete DMEM/F12, with 1% streptomycin-penicillin (Gibco), 0.5% Nonessential amino acids (HyClone), and 10% fetal bovine serum (FBS; HyClone). 143B and Saos-2 cells were cultured in DMEM with 1% penicillin-streptomycin, 10% FBS, and 1% L-glutathione (Gibco). All the cell lines were incubated under 5% CO2 atmosphere at 37°C, unless otherwise indicated. All the chemical agents were provided by Sino-pharm Chemical Reagent Company (Beijing, China), unless otherwise indicated. Recombinant human TRAIL was provided by Thermofisher Corp (Waltham, MA, USA) and reserved in PBS+0.01% BSA at -20°C.

2.2. Dosage Information. The TMS concentration used in this study ($2.5, 5, 10\,\mu$M) for *in vitro* experiment was referred to previous studies. For control group, 1% DMSO were used as a vehicle [18, 19]. The TMS concentration used for *in vivo* experiment on mice was calculated according to the previous publications, which was 11 times as much as that for human beings [20]. This dosage is accomplishable for humans by available supplements via taking orally. Mice were pretreated with TMS (10 mg/kg) by intragastrical gavage every two days; 1% Dimethyl sulfoxide (DMSO) were used as a vehicle in control group. To evaluate the potential toxicity of TMS (10 mg/kg) *in vivo*, the results on kidney and liver function and the blood cell counts in mice were detected by commercial kits.

2.3. Cell Viability. Cell viability was analyzed using trypan blue staining assay kit (Sigma, USA) and 3-(4,5-dimethyl-thiazol-2-yl)-2,5-diphenyltertrazolium bromide tetrazolium (MTT) assay (Sigma, USA). For trypan blue staining assay, 2×10^5 cells were cultured into 48-well plates after treatment for 24 hour. The cell viability was assessed after mixing $200\,\mu$L of cell suspension and $200\,\mu$L of 0.5% trypan blue solutions (Sigma, USA), and the cell counting was performed with a Neubauer chamber. The average of three readings for each group was counted, and the cell count was calculated based on the following equation: number of cells/mL = average cells count $\times 2 \times 10^5$. For MTT assay, $10\,\mu$L MTT solution was added into the medium (2×10^4 cells/well) and incubated at 37°C for 3.5 h. Then, the MTT mixture was discarded, and $100\,\mu$L DMSO was added. After agitating for 20 min, the absorbance of each sample at 570 nm was detected by a microplate reader (Bio-Rad, USA).

2.4. Western Blot Assay. Cells were extracted with lysis buffer for obtaining total proteins. The proteins were transferred to PVDF membrane after separating on 4% SDS-PAGE. After blocking with 4% de-fat milk for 1.5 hour at 25°C, the membrane was washed with TBST for 2 times and following with the primary antibody incubation at 5°C for 12 hour. Then, the membrane was washed with TBST for 2 times and further incubated with secondary antibodies for 1.5 hour at 25°C. The protein blots were visualized by using an ECL system and quantified with ImageJ software (National Institutes of Health, USA). Actin was used as a loading control for normalizing the bands density. The information of primary antibodies used in this study are shown below. Caspase-8 (ab 20421), caspase-3 (ab13847) at dilutions 1 : 500, caspase-9 (ab2154) at dilutions 1 : 500, p53 (ab131162) at dilutions 1 : 1000, H2A.X (ab141768) at dilutions 1 : 200,

phospho-H2A.X (ab 51272) at dilutions 1 : 200, and PARP-1 (ab12633) at dilutions 1 : 1000 were purchased from Abcam (Cambridge, USA). The primary antibody for actin (CS4970) at dilutions 1 : 200 was purchased from Cell Signaling Technology (Trask Lane Danvers, USA); PUMA (sc-41606) and Bax (sc-43716) were provided by Santa Cruz Biotechnology (Santa Cruz, USA) that were used at dilutions 1 : 500 and 1 : 1000.

2.5. Apoptosis Assessment by DAPI Staining and TUNEL Assay. Osteosarcoma cells were cultured in a 40-dish at 5×10^4 cells/mL, stabilized for 12 hours, processed with TMS at different concentrations, then, cultured in an incubator for 12 hours. Nuclear fragmentation and condensation were examined by 4,6-diamidino-2-phenylindole (DAPI) staining. After incubation with TMS, the cells were harvested, washed, and resuspended in PBS, stained with 1 μg/mL DAPI and placed at 4°C with a cover slip, protected from light for 25 min. Then, the samples were washed three times with PBS and examined by fluorescence microscopy.(Thermo Scientific, USA). For TUNEL assay, paraffin-embedded cancer tissues were examined by TUNEL commercial kit (Invitrogen, USA). Briefly, cells were fixed with 4% paraformaldehyde for 10 min at 25°C and then washed with PBS twice. Paraffin tissue sections were processed with 20 μg/mL proteinase K for 5 min. Then, the samples were treated with the 3% H2O2 for 15 min and incubated with 10 μL TdT enzyme reaction buffer for 1 hr at 37°C. The digoxigenine-dUTP end-labeled DNA was examined by antidigoxigenin peroxidase antibodies (1 : 200; ROCHE, Swiss) following the manufactures instructions. *In vivo* fluorescence imaging quantification was analyzed on images captured using confocal microscopy (Olympus, Japan).

2.6. ROS Generation Assessment. Intracellular ROS in osteosarcoma cell was detected using CM-H2DCDFA, which is an uncharged and nonfluorescent ROS indicator. Briefly, 100 μg of CM-H2DCDFA (Life Technologies, USA) was added into each sample. The cells were harvested 25 minutes after CM-H2DCDFA incubation and kept in -80°C. Then, the cells were fixed with 5% PFA/PBS at 4°C for 10 min. After washed by PBS for twice, cells were detected under a fluorescent microscope (400x magnification). Both captured fluorescence and gray images were evaluated by DP controller 3.0 (Leica, Germany). Gray images for analyzing fluorescence intensity were processed by Image J 2.0.

2.7. DNA Comet Assay. To detect single- and double-stranded DNA breaks, DNA comet assay was performed in our study. The pretreated osteosarcoma cells were immersed in fresh lysing solutions in dark place at 4°C for 2 hours and then rinsed with neutralization buffer (200 mM Na2EDTA, 10 mM Tris-HCl, 3 M NaCl, 1% Triton X-100, and 9% DMSO) to eliminate salts and detergents. The samples were set in horizontal electrophoresis system at 5°C with alkaline buffer for 25 minutes (20 V, 250 mA), which promotes the damaged DNA to deviate from the nucleus. Then, the agarose gel was stained with ethidium bromide (20 μg/mL) (Vista Green, USA) for 15 minutes in dark. The slides were

Table 1: Sequences for siRNA transfection.

Gene bank ID	Gene name	siRNA sequences
AG072923	*PUMA*	F: 5′-CUCCAAACUGCGAUGACUU-3′ R: 5′-UAUCUCACAACGGCACGAC-3′
AK356651	*P53*	F: 5′-GUGCACCGGCUCUACAAUA-3′ R: 5′-ACUUACGGCAGCUCAGACC-3′

visualized using an epifluorescence microscope (ZEISS AXIOS A1, Germany) with a magnification of 400x, using a 580 nm filter. Tail moment was evaluated via calculation of percentage of tail length × tail DNA.

2.8. siRNA Transfection. siRNA targeting *p53* or *PUMA* were transfected into 143B cells based on the manufacturer's manual. Generally, siRNA (20 nM) against *p53* or *PUMA* (Table 1) was transfected with RNAiMAX transfection reagent (Invitrogen, USA) into 143B cells for 36 hours at 36°C. Cells were then washed with PBS, and the efficiency of transfection was validated by Western blotting.

2.9. Orthotopic Transplantation Tumor Model of Osteosarcoma. The female BALB/c-nu/nu nude mice (4-week-old) were purchased from the Experimental Animal Centre in University of Kansas (Kansas, USA), and the mice were treated according to the ethics committee's guidelines and regulations under the project license No. K8139B5G. The mouse was fed with standard diet. Before the surgical procedure, anesthesia was induced with 2.5% isoflurane and O2 at 2–4%. Osteosarcoma 143B cells were diluted in PBS (1×10^6 cells/mL) and 200 μL of cell suspension were injected to the tibial plateau of mouse. Then, nude mice were randomly divided into four groups ($n = 5$): TMS (1 μg/g), TRAIL (100 ng/g), TRAIL (100 ng/g) + TMS(1 μg/g), and control group (0.1% DMSO +PBS). Tumor volume and body weight were measured every 7 days. At the end of the experiment, the mice were sacrificed with carbon dioxide, and the tumors were dissected for further analysis. The blood was collected from the tail vein to assess kidney and hepatic function.

2.10. Immunohistochemistry. The mice' osteosarcoma tissue sections (5 μm thick) were dewaxed in xylene for 10 min; then, the samples were rehydrated with alcohol and wished by distilled water. 20 mM citrate buffer was used to process the tissue sections at 96°C for 15 min; fixative was applied to fix the samples. Next, the slides were blocked with 5% BSA for 45 min. Then, the slides were incubated with PUMA (1 : 2000, Abcam) and p53 (1 : 500, Abcam) antibodies at 4°C for 12 h, followed by incubation with secondary antibodies 24°C for 2 h. After washing by PBS, the samples were stained with hematoxylin and DAB. Finally, the slides were examined with a fluorescence microscope, and the brown color indicated the positive cells.

2.11. Statistics. One-sample *t*-test was applied for quantification of the band intensity of Western blotting, the two-

sample t-test was used for analyzing the means of two groups, and one-way ANOVA with Dunnett's multiple comparison was used to compare the means among more than two groups. Data are expressed as the mean ± standard deviation (SD). The data is considered as significant difference when $P < 0.05$.

3. Results

3.1. TRAIL Resistance in Osteosarcoma 143B Cells.

To examine TRAIL resistance in osteosarcoma cell lines, 143B and Saos-2 cells were treated with 0-200 ng/mL TRAIL for 12 h. Our results indicate that 50-200 ng/mL TRAIL suppressed the viability of Saos-2 cells in a dose-dependent manner (Figures 1(a) and 1(b)). However, the viability of 143B cell was not significantly changed after TRAIL treatment; the survival of 143B cells was about 92% when pretreated with TRAIL (200 ng/mL). Cleaved poly (ADP-ribose) polymerase-1 (PARP-1), an indicator of apoptosis, was detected in Saos-2 cells only (Figures 1(a) and 1(b)). We then used DAPI staining and TUNEL labeling to determine whether apoptosis occurred after the cell was pretreated by 100 ng/mL TRAIL. DAPI staining results show chromosome condensation in Saos-2 cell after TRAIL treatment (100 ng/mL), while no significant subcellular morphological changes were detected in 143B cells pretreated with 100 ng/mL TRAIL (Figure 1(c)). The results of TUNEL assay were consistent with those obtained using DAPI staining. These results suggest that TRAIL-treated Saos-2 cells were sensitive, while TRAIL-treated 143B cells were resistant, to apoptosis.

3.2. The Effect of TMS on TRAIL-Resistant Osteosarcoma Cells.

Next, we examined whether a noncytotoxic dose of TMS could induce apoptosis in 143B cells. For this, 143B cells were exposed to 0–10 μm TMS for 6 h, and then, cellular viability was examined using the Trypan blue dye exclusion method. Our results demonstrate that treatment with 2.5 μm TMS alone did not inhibit the survival of 143B cells (Figure 2(a)). However, cotreatment using TRAIL (50 ng/mL) and TMS (2.5 μm) for 6 hours did inhibit the survival of 143B cells (Figure 2(b)). Western blotting showed that the levels of PARP-1 cleavage were not increased in 143B cells after treating by 1–5 μm TMS or TRAIL (50 ng/mL). However, cotreatment with 2.5 μm TMS and 50 ng/mL TRAIL increased the expression of cleaved PARP-1 in 143B cells (Figure 2(c)). Interestingly, combination therapy by 2.5 μm TMS and 50 ng/mL TRAIL did not induce PARP-1 cleavage in normal human hFOB1.19 osteoblasts (Figure 2(d)). Furthermore, DAPI and TUNEL labeling confirmed that combined treatment using TRAIL and TMS did induce apoptosis in 143B cells (Figure 2(e)).

3.3. Cotreatment with TMS and TRAIL Activates Caspases Signaling.

To explore the mechanisms underlying TMS- and TRAIL-induced apoptosis in 143B cells, we assessed the expression of cleaved PARP-1 and several caspases in 143B cells treated with TMS and/or TRAIL. No significant changes in the expressions of cleaved PARP-1 or caspases were observed in 143B cells treated with TMS or TRAIL alone (Figure 3(a)). However, cotreatment using TMS (2.5 μm) and TRAIL (50 ng/mL) induced PARP-1 and caspase cleavage in a time-dependent manner (Figure 3(a)). Caspase cleavage was enhanced by TMS in a dose-dependent manner (Figure 3(b)). Next, we used different caspase inhibitors, including zlEHDfmk, zlETDfmk, and zDEVDfmk, to evaluate the possible roles of caspase cleavage in the survival of 143B cell cotreated with TMS and TRAIL. Our results show that PARP1 cleavage and apoptosis in 143B cells were inhibited by treatment with caspase inhibitors (Figure 3(c)). Together, these data suggest that cotreatment with TRAIL and TMS activated caspases and induced apoptosis in 143B cells.

3.4. TMS Increases Intracellular ROS Levels in 143B Cells.

Reactive oxygen species (ROS) and mitochondria play important roles in the induction of apoptosis under conditions of physiologic and pathologic stress. Thus, we evaluated intracellular redox status in 143B cells after treatment with TMS and TRAIL. A CARBOYX-H$_2$DCFAD fluorescence probe was used to detect intracellular ROS levels in treated 143B cells. Our results show that 143B cells treated with positive control (H$_2$O$_2$) or 2.5 μm TMS emitted stronger fluorescent signal compared with that of the control group (Figure 4(a)). Results obtained using spectrofluorometry indicate that relative fluorescence intensity was increased in 143B cells after treatment with TMS, suggesting that TMS may have increased ROS levels in a dose-dependent manner (Figure 4(b)). Relative fluorescence intensity reached peak level 20 minutes after the cells received the recommended dose of TMS (2.5, 5 μm). Sixty minutes after reaching its peak level, relative fluorescence intensity rapidly decreased to its minimal value. Interestingly, 4 h after reaching its minimal value, relative fluorescence intensity increased again (Figure 4(c)). These results indicate that TMS may regulate intracellular ROS generation in 143B cells in biphasic pattern. For further exploring the possible roles of ROS in TRAIL- and TMS-mediated apoptosis of 143B cells, NAC (which is an ROS inhibitor) was used to treat 143B cells after treatment with TRAIL and/or TMS. Our results show that TRAIL (50 ng/mL) had no effect on intracellular ROS levels, while NAC (4 mM) reduced ROS level induced by TMS (Figure 4(d)). Additionally, NAC reversed the cellular apoptosis that had been induced by cotreatment with TMS and TRAIL in human 143B cells (Figure 4(e)). These results indicated that when ROS was inhibited by NAC, the proapoptotic effect of TMS and TRAIL could be attenuated. The P53 protein exerts dual effects under conditions of intracellular oxidative stress, providing cytoprotection at basal ROS levels and inducing senescence/apoptosis at high ROS levels [21]. Previous studies have shown that TMS-mediated cellular apoptosis is associated with increased expression of p53 and PUMA in osteosarcoma cells [22]. Thus, we used immunoblotting to detect the expression of cleaved PARP-1, p53, and PUMA in 143B cells cotreated with TMS and TRAIL. Our results show that combined treatment with TMS and TRAIL upregulated the expressions of cleaved PARP1, PUMA, and p53 in 143B cell. Interestingly, NAC (4 mM)
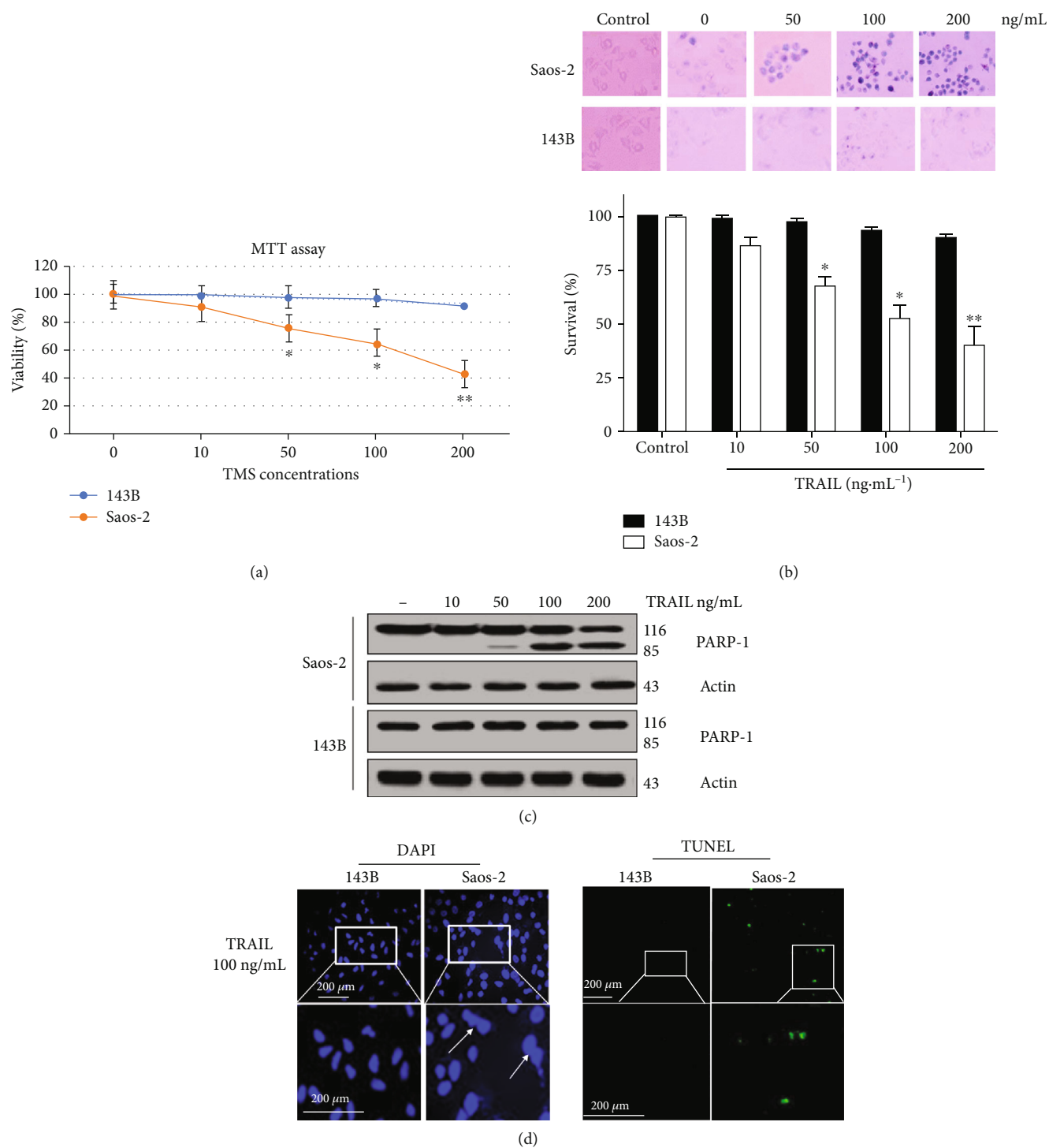
(a)

(b)

(c)

(d)

Figure 1: TRAIL suppresses viability and promotes apoptotic cell death in Saos-2 cells. MTT assay (a) and Trypan blue staining (20x objective lens) (b) were used to examine the survival of 143B and Saos-2 cells after treatment with 0–200 ng/mL TRAIL for 12 h. Equal volume of vehicle (0.01% BSA + PBS) was used to treat the control groups, $^{*}P < 0.05$; $^{**}P < 0.01$. (c) Western blotting was used to detect PRAP-1 cleavage in 143B and Saos-2 cells treated with 0–200 ng/mL TRAIL for 6 hour. (c) DAPI and TUNEL labeling were used to examine apoptosis in 143B and Saos-2 cells treated with 100 ng/mL TRAIL for 6 hours. White arrows indicate chromatin condensation in 143B and Saos-2 cells; spots of green fluorescence indicate morphological changes in 143B and Saos-2 cells (magnification ×200); additional higher-magnification images are also provided (magnification ×400).

reversed the effects of TMS and TRAIL on protein expression of cleaved PARP1, p53, and PUMA (Figure 4(f)). These findings indicate that combined treatment with TRAIL and TMS

induced ROS generation in 143B cells and promoted intrinsic apoptotic signaling by upregulating the expression of p53 and PUMA.

(a)

(b)

(c)

(d)

(e)
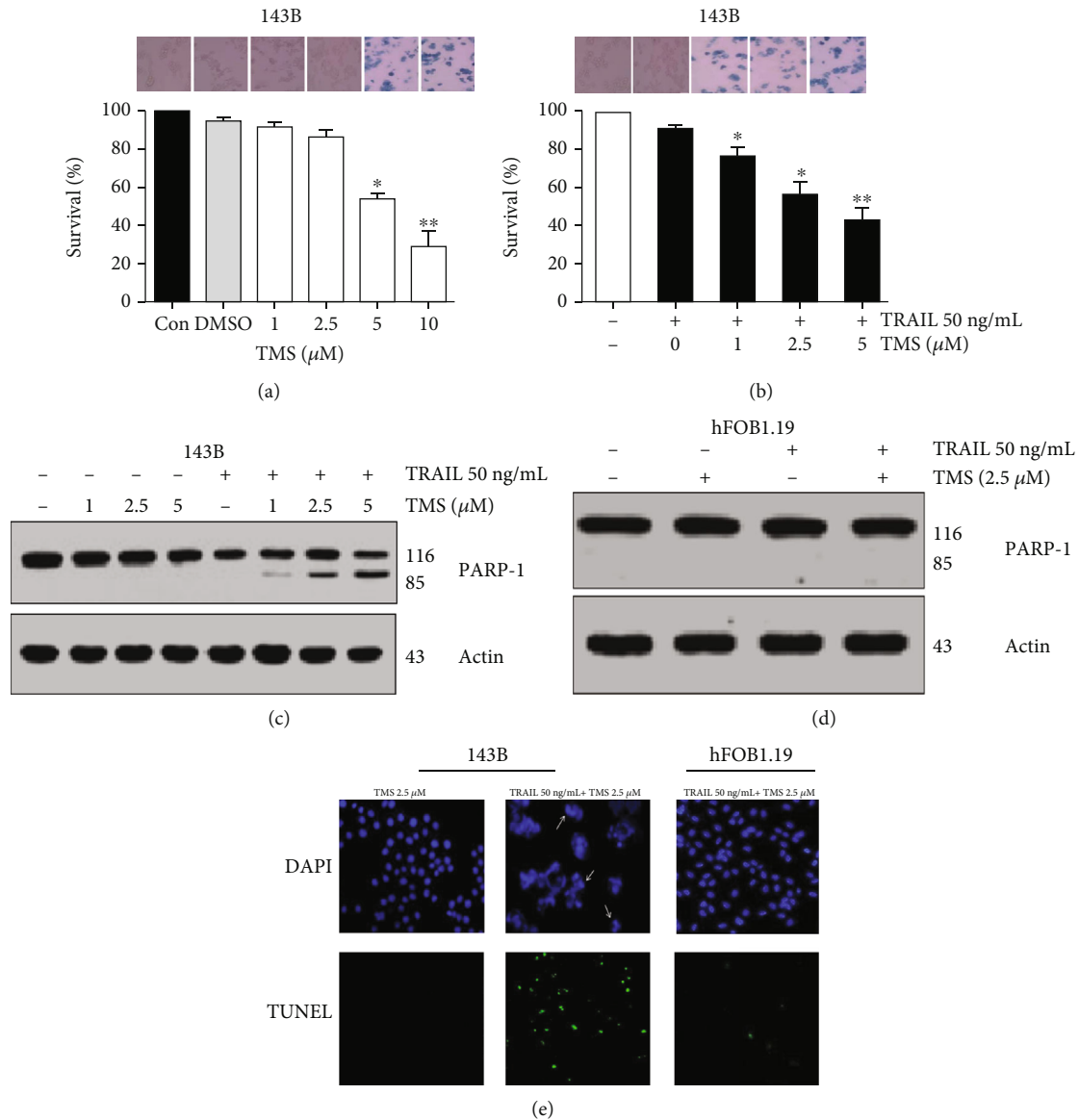
FIGURE 2: TMS reverses TRAIL-resistance in 143B cells. (a) After treatment with different doses of TMS for 6 h, the survival rate of 143B cells was examined using the Trypan blue dye exclusion method (20x objective lens). (b) Survival of 143B cells, treated with 0–10 μm TMS and/or 50 ng/mL TRAIL, was assessed using the Trypan blue dye exclusion method. (c) Human osteosarcoma 143B cells and (d) normal human hFOB1.19 osteoblasts were pretreated with 50 ng/mL TRAIL and 2.5 μm TMS for 10 hours. Western blotting was used to detect the levels of cleaved PARP1. (e) DAPI and TUNEL labeling were used to evaluate the apoptosis of 143B osteosarcoma cells and normal hFOB1.19 osteoblasts after treatment with TMS and/or TRAIL for 6 h (magnification ×400).

3.5. TMS Induces DNA Damage in 143B Cells. ROS-induced oxidation of DNA is one of the major causes of gene mutation, resulting in various types of DNA damage such as double-strand breaks in the chromosome. DNA damage may result in apoptosis [23]. To examine the DNA damage potentially caused by exposure to TMS, we performed a comet assay to detect double-strand breaks in the chromosomes of TMS-treated 143B cells. Results of the comet assay indicate that the length of DNA migration (tail length), which reflects the extent of DNA damage, was increased in 143B cells treated with TMS (2.5 μM) (Figure 5(a)). These results show that TMS may have induced DNA damage and consequent apoptosis in 143B cells. H2AX is phosphor-

ylated on serine 139 and is then designated as γH2AX in a reaction involving DNA double-strand breaks [24, 25]. Therefore, the expression of H2AX and phosphorylation of H2AX-Ser139 were examined to confirm that treatment with TMS induced DNA damage in 143B cells. Our results indicate that TMS facilitated H2AX-Ser139 phosphorylation in 143B cells in a dose- and time-dependent manner (Figures 5(b) and 5(c)). Above data suggest that TMS may activate P53 and trigger apoptosis by increasing ROS levels and inducing DNA damage in 143B cells.

3.6. TMS Activates p53 and PUMA Expression in Osteosarcoma Cells. Previous studies have confirmed that
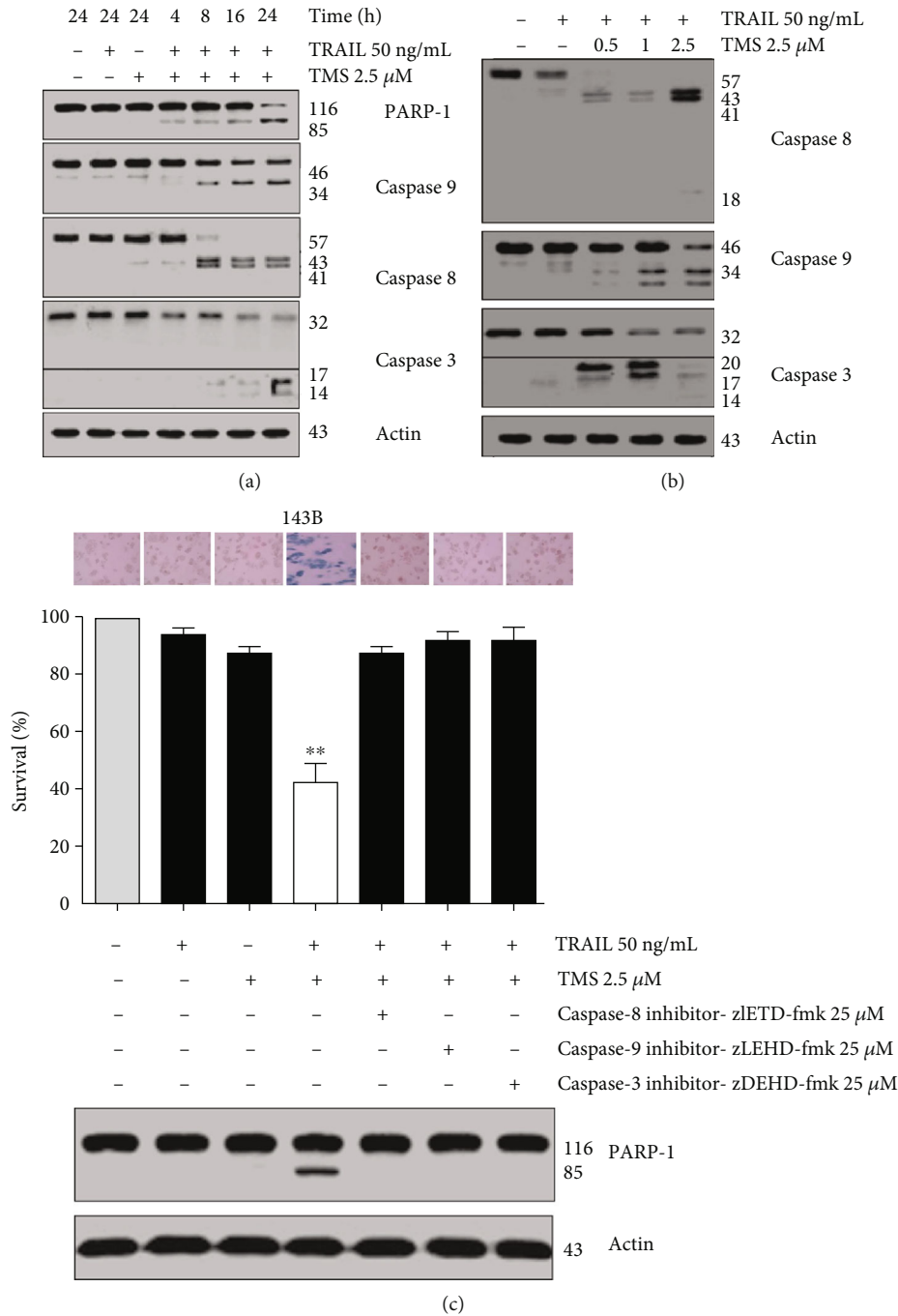
(a)

(b)

(c)

Figure 3: Cotreatment with TRAIL and TMS can activate caspases in 143B cells. (a) Western blotting was used to detect the expression of PARP-1 and caspase cleavage in 143B cells treated with TMS and/or TRAIL for different lengths of time. The control group was treated with an equal volume of 1% DMSO + PBS+0.01% BSA. (b) Caspase cleavage was examined by Western blotting in 143B cells after treatment with 50 ng/mL TRAIL and TMS (0.5–2.5 μM) for 10 hours. (c) Caspase inhibitory agents, including zlEHDfmk, zlETDfmk, and zDEVDfmk, were used to block the caspase pathway in 143B cells. After the cells were pretreated with TMS and/or TRAIL for 10 hours, the Trypan blue dye exclusion method was used to evaluate cell survival (20x objective lens), and Western blotting was utilized to detect the expression of cleaved PARP1. $^{**}P < 0.05$.

p53 phosphorylation may affect its stabilization in cells [26]. In our study, we found that TMS could activate P53 by phosphorylation of P53 on Ser15, Ser46, and Ser392; this activity was crucial for p53 accumulation and stabilization in 143B cells (Figure 6(a)). As a downstream target gene of p53, *PUMA* is upregulated by p53 activation and can induce apo-

ptosis in cells exposed to TMS [22]. In this study, we further examined the roles of p53 and *PUMA* in the apoptosis of 143B cells after cotreatment with TMS and TRAIL. Figure 6(b) shows that TMS dose-dependently upregulated the expression p53 and PUMA. After cotreatment with TMS (1–5 μM) and TRAIL (50 ng/mL), the expression of
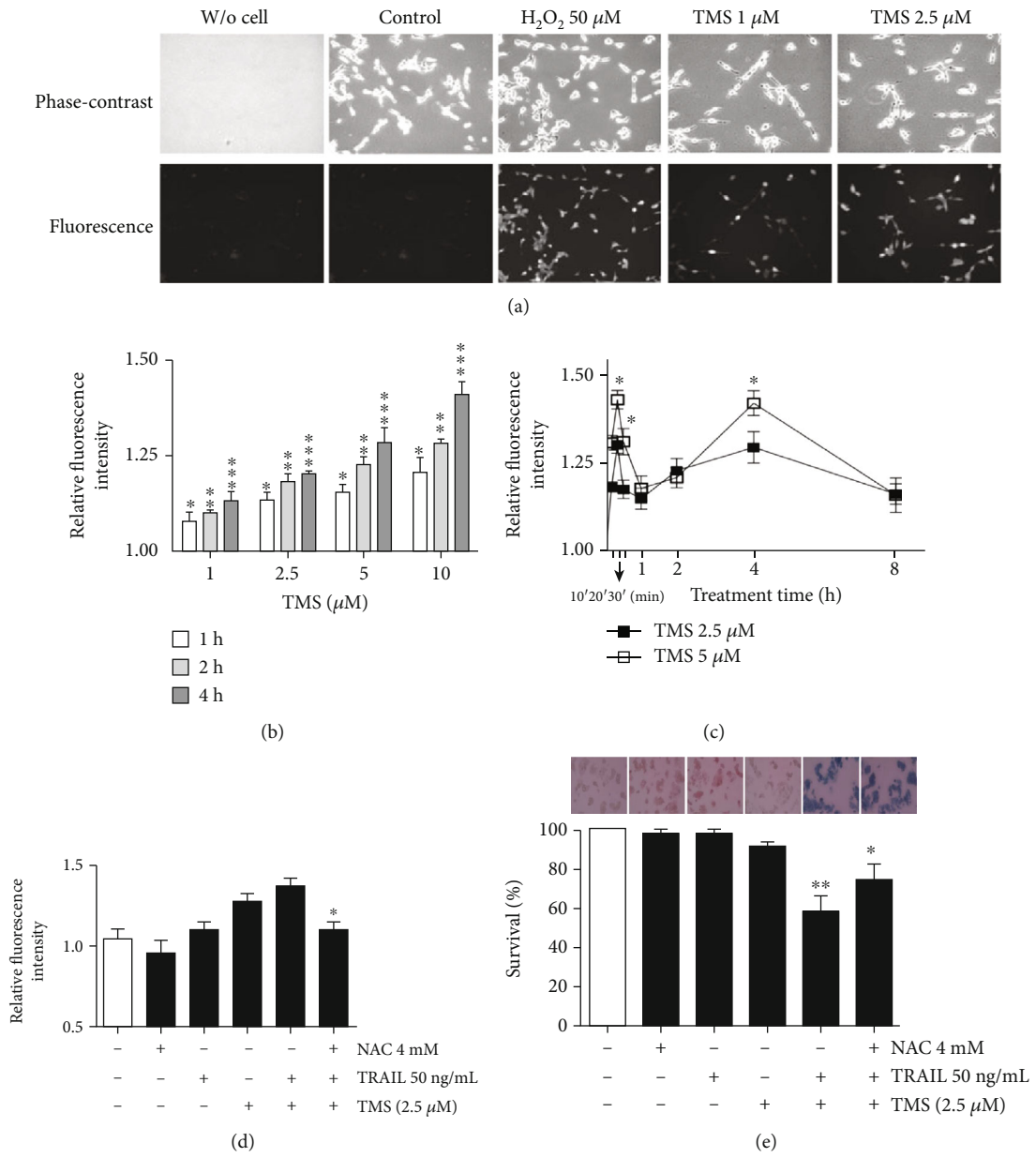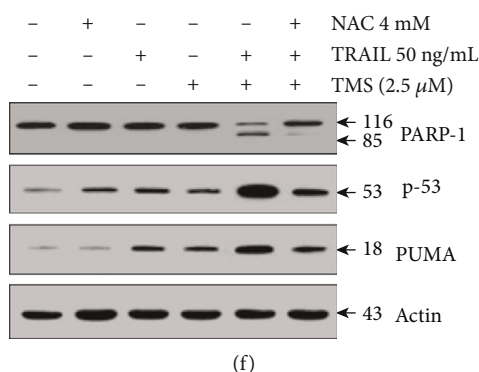
(a)

(b)

(c)


(d)

(e)

Figure 4: Continued.

(f)

Figure 4: TMS increases ROS levels in 143B cells. (a) Intracellular ROS levels in 143B cells were detected using fluorescence microscopy. The cell was pretreated with positive control (H_2O_2) or TMS for 50 minutes and labeled with CMH2DFCDA for 15 minutes. Considerably higher fluorescence intensity was detected in cells treated with H_2O_2 or TMS compared with that of the 0.01% BSA+ PBS-treated control group. (b) 143B cell was pretreated with different doses of TMS for various periods of time. ROS generation was measured using relative fluorescence intensity in 143B cells. $^{**}P < 0.05$. (c) After treatment with TMS (2.5, 5 μm) for various periods of time, 143B cell was labeled with CMH2DFCDA. ROS levels were analyzed at different time points according to the value of relative fluorescence intensity. (d) Pretreatment with NAC reduced ROS generation induced by TMS (2.5 μm) and (e) attenuated TMS- and TRAIL-induced apoptosis in 143B cells. Trypan blue dye exclusion method was used to evaluate cell survival (20x objective lens). $^*P < 0.05$; $^{**}P < 0.01$. Cells in the control group were treated with an equal volume of PBS+0.1% DMSO. (f) Immunoblotting were used for examining the expression of cleaved PARP-1, p53, and PUMA in 143B cells after pretreatment with NAC and treatment with TRAIL and TMS.
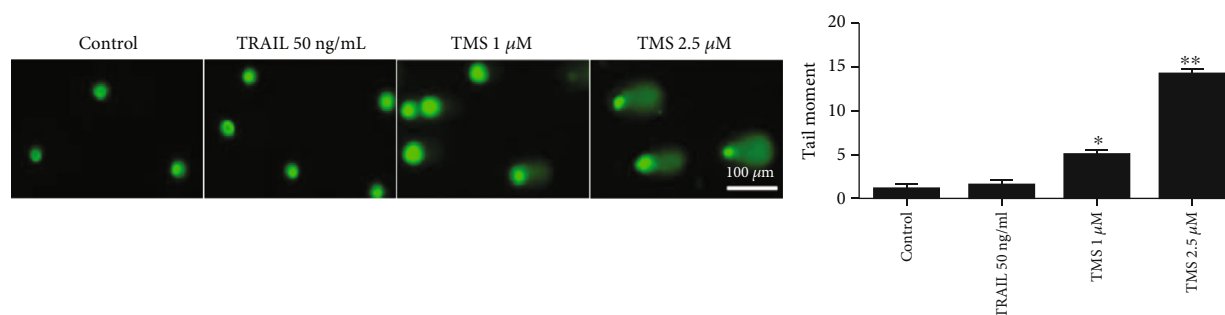
(a)
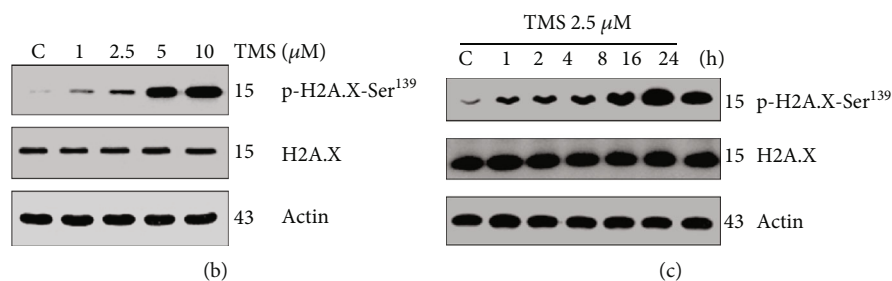
(b)

(c)

Figure 5: TMS induces DNA damage and facilitates phosphorylation of Ser-139 (H2AX) in 143B cells. (a) Comet assay was performed to examine DNA damage induced by treatment with TMS or TRAIL for 15 minutes. Tail moment were applied for quantifying double-strands break via calculating the tail length × percentage of tail DNA. $^*P < 0.05$. (b) 143B cell was treated with 0–10 μM TMS for 24 hours, and Western blotting was used to examine the expression of H2AX and phospho-H2AX-Ser139 in 143B cells; 0.01% DMSO was used as vehicle control. (c) 143B cell was pretreated with TMS (2.5 μM) for 0-24 hours, and immunoblotting was used to examine the expression of H2AX and phospho-H2AX-Ser139 expression in 143B cells; 0.01% DMSO was used as vehicle control.

PUMA and p53 was significantly increased in 143B cells (Figure 6(c)). RNA interference assay was used for downregulating the expressions of PUMA and P53 in order to confirm the critical roles of PUMA and p53 in TMS-mediated sensitization of 143B cells to TRAIL stimulus. Our results indicate that 48 h after transfection with PUMA or p53 siRNA, cleaved PARP-1 expression was significantly

decreased in 143B cells, which suggests that TMS-induced TRAIL sensitization was attenuated in p53- or PUMA-silenced cells (Figure 6(d)). DAPI staining confirmed that transfection with PUMA or p53 siRNA reversed apoptosis in 143B cells after cotreatment with TRAIL and TMS (Figure 6(e)). These findings suggest that activation of p53 and PUMA contributed to TMS-mediated TRAIL
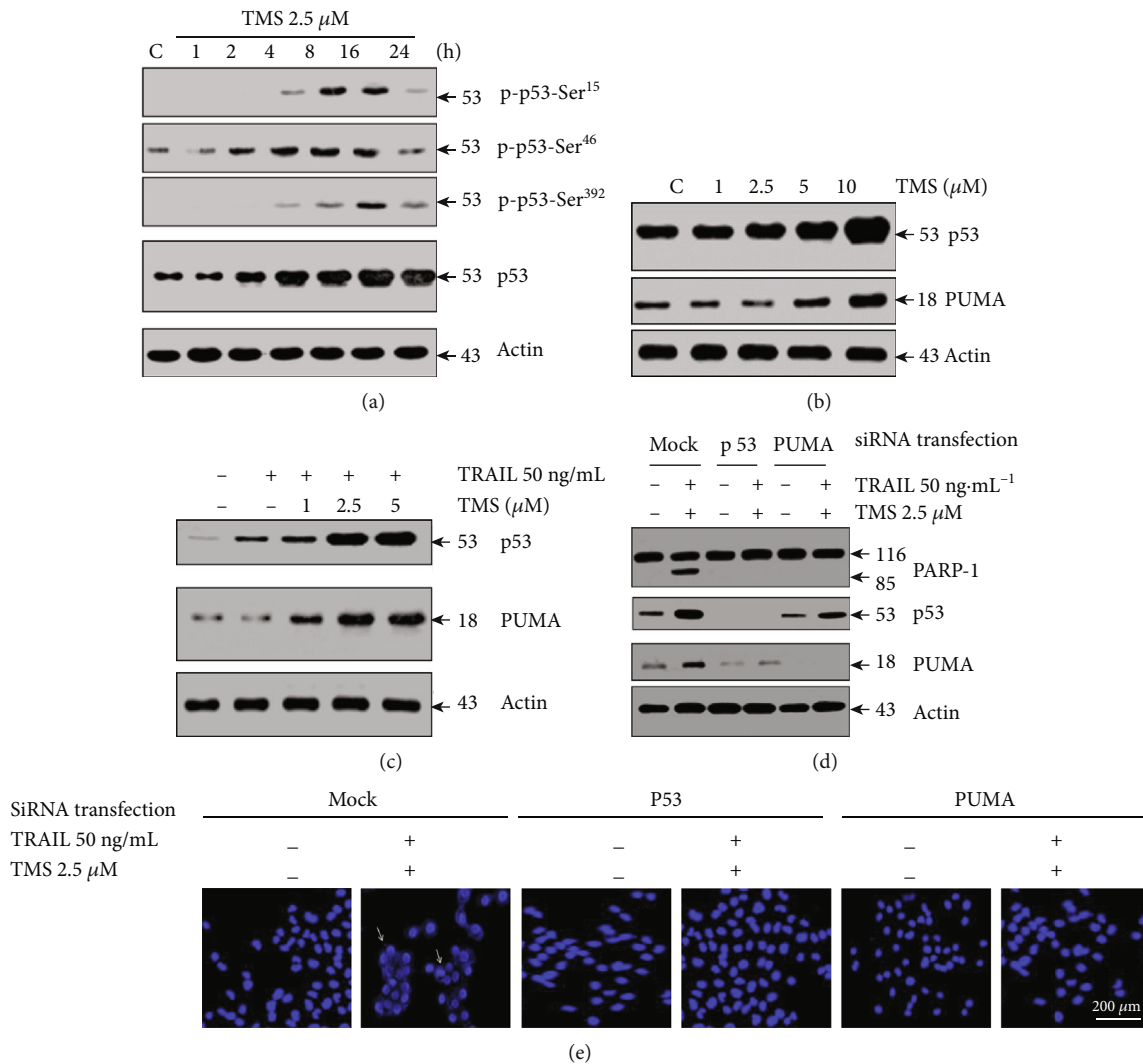
Figure 6: TMS activates PUMA and p53 expression in osteosarcoma cells. (a) TMS (2.5 μM) was used to treat 143B cells for 0–24 h, and protein expression of phosphorylated p53 (on Ser392, Ser46, or Ser15) was examined by Western blotting; 0.01% DMSO was used as vehicle control. (b) Different doses of TMS were used to treat 143B cells for 10 h, and Western blot assay was performed to detect the expressions of P53 and PUMA. (c) Different doses of TMS and TRAIL were used to treat 143B cells for 10 h, and Western blot assay was performed to detect the expressions of P53 and PUMA. (d) Gene expression of *p53* and *PUMA* was silenced by siRNA in 143B cells, and then, the cells were treated with TRAIL and TMS for 10 h. Western blotting was used to examine the expression of cleaved PARP1, P53, and PUMA. (e) Apoptotic cells were examined by DAPI staining after treating *p53-* or *PUMA*-silenced 143B cells with TMS and TRAIL. White arrows indicate condensed chromatin in 143B cells (magnification ×400).

sensitization and apoptosis in 143B cells. Next, we used MG-63 cells, another osteosarcoma cell line, for further verifying the effect of p53 in TMS- and TRAIL-induced apoptosis of osteosarcoma cells. Two strains of MG-63 cells, p53−/− and p53+/+, were treated using 2.5 μM TMS + TRAIL (50 ng/mL) for 0-24 h. Figures 7(a) and 7(b) show that TMS inhibited the viability of MG-63 p53+/+ cells and increased the expression of cleaved PARP-1. However, MG-63 p53−/− cells were not sensitive to treatment with TMS. Two other MG-63 cell lines (MG-63 PUMA+/+ and MG-63 PUMA−/−) were used to assess the role of PUMA in TRAIL- and TMS-induced apoptosis of osteosarcoma cells. Figures 7(c) and 7(d) show that TMS may have induced sensitization to TRAIL-induced apoptosis and increased the expression of cleaved PARP-1 in

MG-63 PUMA+/+ cells, while MG-63 PUMA−/− cells were not sensitive to the combined treatment. These results suggest that activation of PUMA or p53 was involved in TMS-mediated sensitization of osteosarcoma cells to TRAIL-induced apoptosis.

3.7. The Impact of BAX in TMS- and TRAIL-Mediated Apoptosis.
BAX is a key member of the antiapoptotic Bcl-2 family, which plays critical roles in the apoptosis of tumor cells. The coordinated activity of Bax and its upstream activators (PUMA and p53) can promote mitochondrial activation and apoptosis [27]. We next used 143B Bax+/− and 143B Bax−/− cells to confirm the role of Bax in TMS- and TRAIL-induced apoptosis. Our results show that TRAIL-mediated
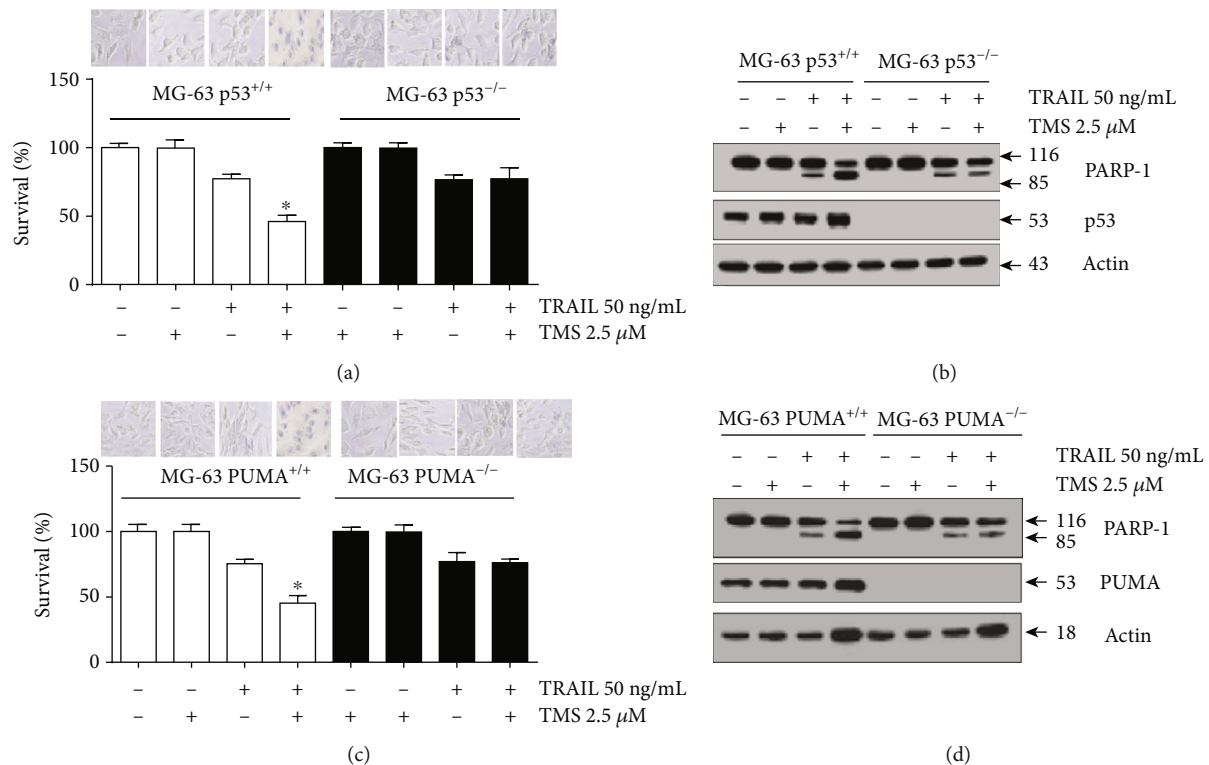
FIGURE 7: Treatment with TMS overcomes TRAIL resistance and promotes apoptotic cell death of MG-63 cell via activating p53 and PUMA. (a) Wild-type MG-63 cell, (b) p53−/− MG-63 cell or (c) wild-type MG-63 cell, and (d) PUMA −/− MG-63 cell were pretreated by TRAIL (50 ng/mL) and TMS (2.5 μm) for 10 h. Equal volume of PBS+0.1% DMSO 0.01% + BSA was used as vehicle control. Cell survival was examined as indicated in the experimental method section. Immunoblotting was used to detect the expression of cleaved PARP1, p53, or PUMA. $^*P < 0.01$.

apoptosis and the expression of cleaved PARP1 were enhanced after 2.5 μm TMS treatment in 143B Bax+/− cells, instead of 143B Bax−/− cells (Figures 8(a) and 8(b)). Combined treatment with TRAIL and TMS significantly increased the expression of PUMA and p53 in both cell types (Figure 8(b)). Morphological assessment of apoptotic osteosarcoma cells by DAPI staining showed nuclear changes and apoptosis in 143B Bax+/− cells when treating by TMS and TRAIL (Figure 8(c)).

3.8. TMS and TRAIL Impair Osteosarcoma Growth In Vivo. A xenograft tumor model using 143B cell was set up in BALB/c mice for evaluating the effects of TMS and TRAIL on osteosarcoma progression. Our results show that tumor weight and volume were reduced in the group treated with TRAIL (100 ng/g) + TMS (1 μg/g) compared with those of the control group. Conversely, no differences in tumor volume or weight were observed between TRAIL (100 ng/g body weight)-treated mice and control mice (Figures 9(a) and 9(b)). The body weights of nude mice in TMS and/or TRAIL groups were similar to those of control-group mice during our *in vivo* studies (Figure 9(b)). Serum levels of alanine transaminase (ALT), aspartate aminotransferase (AST), and those of several renal function markers (creatinine (Cr) and blood urea nitrogen (BUN)) were analyzed in the cardiac blood of nude mice in order to evaluate the potential kidney and liver toxicity of cotreatment with TMS + TRAIL. Our results show that hepatic and kidney function was normal in all the groups of mice used in our study (Table 2). Leukocyte, erythrocyte, and platelet count of the nude mice was also normal, suggesting that cotreatment with TMS + TRAIL exerted no significant hematological adverse effects within the present dosage (Table 3). These results indicate that cotreatment with TRAIL (100 ng/g) + TMS (1 μg/g) inhibited the development of osteosarcoma without significant toxicity in nude mice. Furthermore, the results of immunohistochemistry (IHC) show that the expressions of Bax, PUMA, and p53 were markedly increased in osteosarcoma tissues of TMS + TRAIL treated mice compared with those of the vehicle-treated mice ($P < 0.05$ Figure 9(c)). These results suggest that TMS likely triggers Bax/PUMA/P53 signaling that contributes to intrinsic apoptosis while cotreatment with TRAIL and TMS likely induces extrinsic apoptotic cell death in osteosarcoma.

4. Discussions

The intrinsic and extrinsic apoptosis pathways are naturally occurring or drug-induced processes by which cells are directed toward programmed cell death. Intracellular cues, such as cellular DNA damage, can induce apoptosis primarily via the intrinsic pathway. The intrinsic apoptosis pathway, which involves activation of conserved signaling proteins, such as that of p53, is physically associated with [28]. The
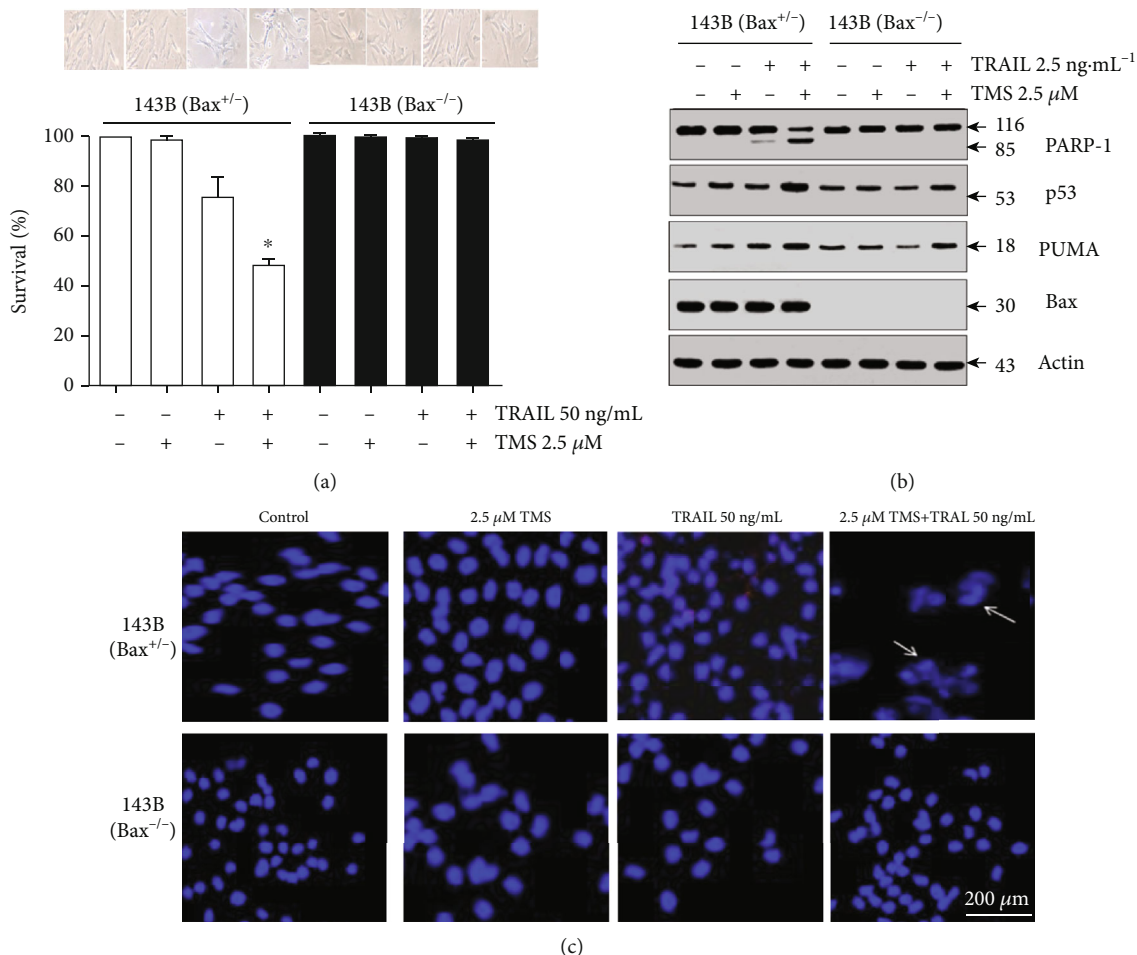
FIGURE 8: The role of BAX in TMS- and TRAIL-mediated apoptosis. (a, b) 143B Bax+/− and 143B Bax−/− cells were exposed to TMS and TRAIL for 10 h. Equal volume of 0.01% BSA + PBS+0.1% DMSO was used as vehicle control. Cell survival rate was analyzed as indicated in the experimental method section. Immunoblotting was used to examine the expression of cleaved PARP1, P53, Bax, and PUMA. $^*P < 0.05$. (c) DAPI was used as specific counterstain for apoptosis to evaluate the effects of cotreatment with TMS and TRAIL in 143B Bax+/− and 143B Bax−/− cells. White arrows indicate chromatin condensation in 143B cells evaluated by fluorescence microscopy (magnification ×400).

extrinsic apoptosis pathway is activated by extracellular ligands binding to cell-surface death receptors, which results in the formation of a death-inducing signaling complex (DISC). Caspases orchestrate both intrinsic and extrinsic apoptotic cell death by activating the cleavage of target proteins [29]. TRAIL, also called TNF superfamily 10, is a pleiotropic cytokine from the tumor necrosis factor superfamily. TRAIL has been shown to selectively induce apoptosis in various tumor cells by activating the extrinsic apoptosis pathway. Treating tumor cells with small molecular inhibitors may facilitate tumor-cell sensitivity to TRAIL-induced apoptosis while exempting normal cells from this fate [30]. Treatments combining TRAIL with small molecular inhibitors, such as the proteasome inhibitor [31], BCL-2 inhibitor [32], mammalian target of rapamycin (mTOR) inhibitor [33], and histone deacetylase (HDAC) inhibitor [34], are being assessed for inhibition of specific signaling proteins that can synergistically facilitate the TRAIL-mediated extrinsic apoptosis pathway. In the present study, our results demonstrate that TMS (used at a noncytotoxic dosage) sensitized

143B cells to TRAIL-mediated apoptosis by increasing the expression of PUMA, p53, and Bax via ROS-induced DNA damage. Mitochondria-mediated caspase-9 activation may have contributed to intrinsic apoptotic signaling induced by TMS by upregulating the levels of intracellular ROS, while death-receptor-mediated caspase 8 activation was likely involved in extrinsic apoptotic signaling triggered by treatment with TRAIL.

TRAIL can selectively induce apoptosis in various cancer cells, as shown in previous studies [12, 35–37]. However, various tumor cells are either intrinsically TRAIL-resistant or become resistant after exposure to TRAIL therapy [38]. Our present results indicate that treatment with TRAIL induced apoptosis in the osteosarcoma cell line Saos-2, while 143B cells showed considerable resistance to TRAIL. These results have consistently agreed with those of previous studies on TRAIL-resistant or TRAIL-sensitive osteosarcoma cell lines [32]. Our results also show that cotreatment using a noncytotoxic dose of TMS and TRAIL promoted apoptosis of 143B cells *in vitro*. These results demonstrate that TRAIL and
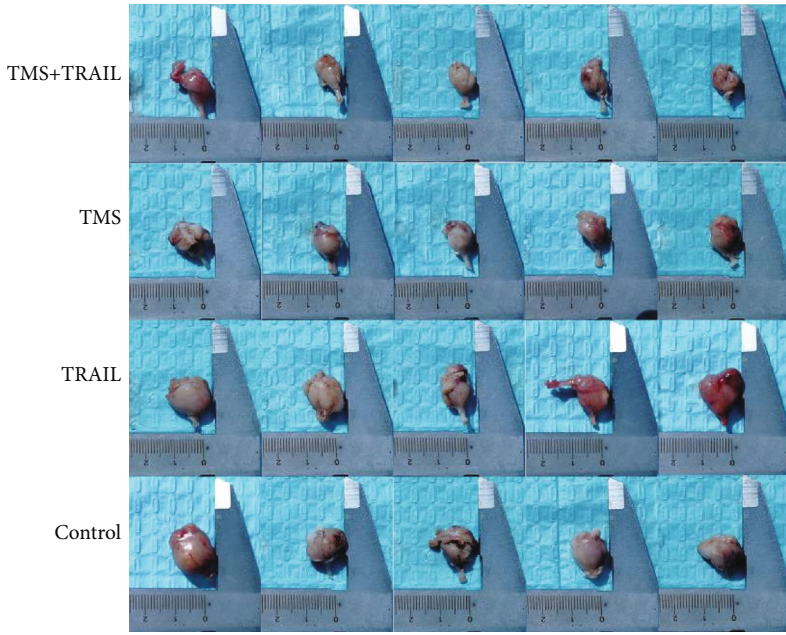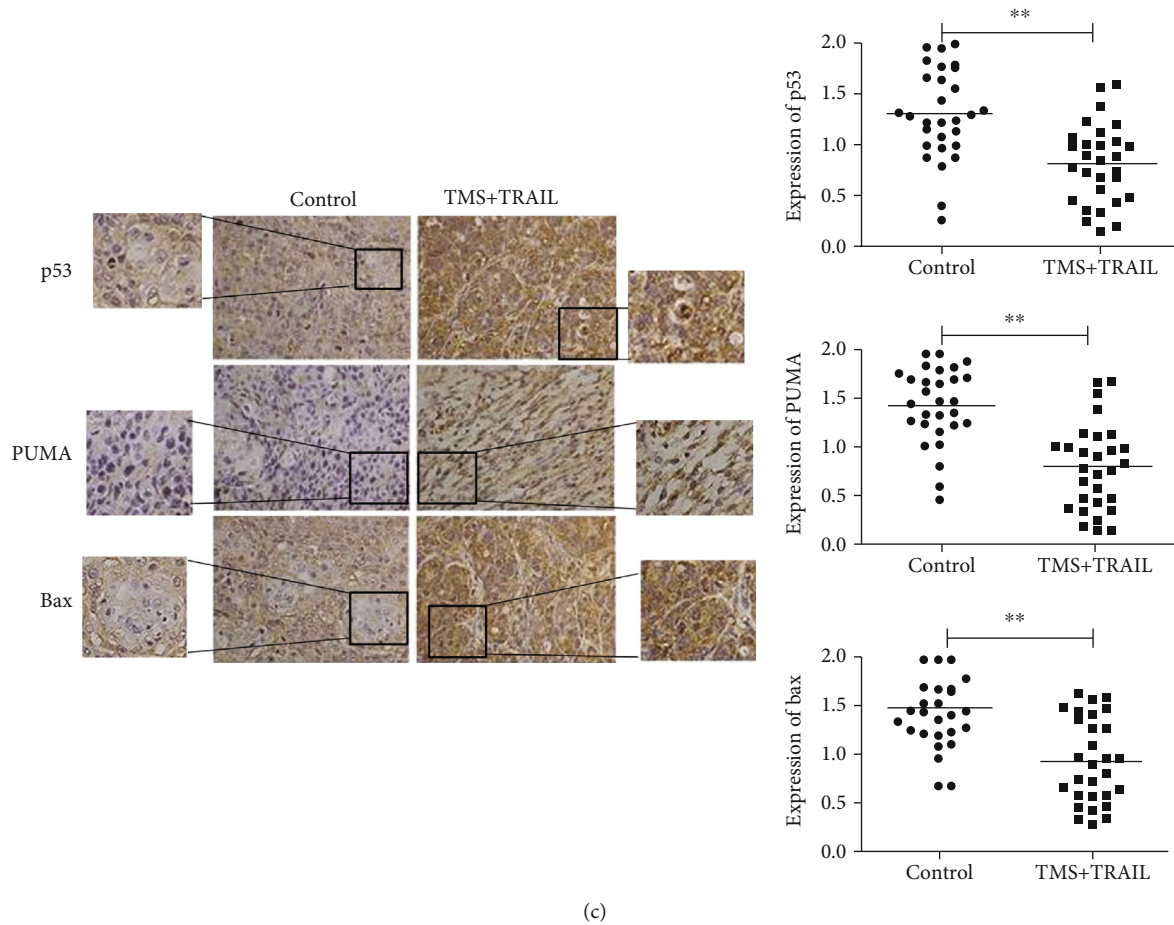
(a)
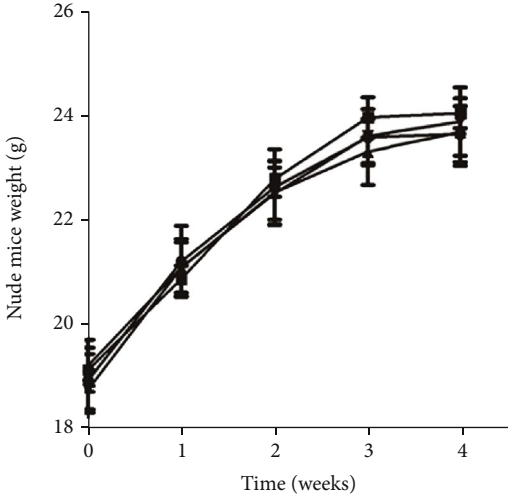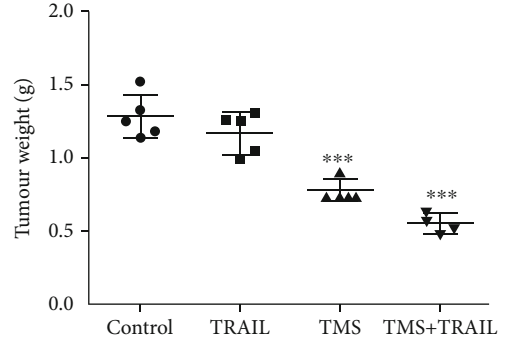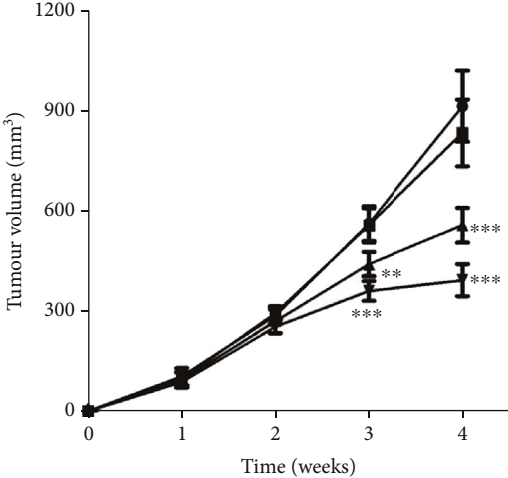
(b)

Figure 9: Continued.

(c)

FIGURE 9: Cotreatment with TMS and TRAIL suppresses the proliferation of cancer cells in nude mice transplanted with osteosarcoma. (a) Sizes of osteosarcoma tumors in nude mice subjected to different treatment regimens. (b) Tumor volume and weight were significantly decreased in TRAIL (100 ng/g) + TMS (1 μg/g)-treated group compared with those of the other groups. No obvious changes in body weight were noted among mice subjected to different treatment regimens. $^{**}P < 0.01$; $^{***}P < 0.001$ versus control. (c) The expression of Bax, PUMA, and P53 was evaluated using immunohistochemistry (IHC). The scored IHC results were analyzed by multiplying the percentages of positive cells by the intensity score obtained using confocal microscopy. Signal intensity was analyzed and scored by two independent pathologists. The score of 0 indicates lack of staining, 1 indicates mild staining, and 2 indicates obvious staining. Osteosarcoma cells in five separate areas were chosen at random and analyzed according to the percentages of positively labeled cells ($^{**}P < 0.01$).

TABLE 2: Effects of TMS + TRAIL on kidney and liver function *in vivo*.

Treatment	Number of mice	Cr (mmol/L)	ALT (μ/L)	AST (μ/L)	BUN (mmol/L)
Control	5	21.13 ± 2.10	31.14 ± 2.01	97.86 ± 9.20	6.19 ± 1.10
TMS	5	21.23 ± 3.30	29.14 ± 3.32	99.14 ± 16.35	5.97 ± 1.01
TRAIL	5	22.42 ± 3.16	28.95 ± 3.35	98.63 ± 12.32	5.76 ± 0.49
TMS + TRAIL	5	22.51 ± 3.67	31.13 ± 3.10	100.34 ± 21.60	5.98 ± 1.86

Cr: creatinine; ALT: alanine aminotransferase; AST: aspartate transaminase; BUN: blood urea nitrogen.

TMS may act synergistically to promote apoptotic cell death in osteosarcoma cell. The opening of the permeability transition pore complex in the membrane of mitochondria is pivotal to cytochrome-C release, apoptosome formation, and subsequent activation of the caspase cascade in intrinsic apoptosis signaling. Caspases, which are intracellular proteases, are responsible for the deliberate disassembly of cell into apoptotic body during apoptotic cell death. Activation of caspases during apoptotic cell death leads to cleavage of critical cellular substrates, such as lamins and poly(ADP-ribose) polymerase, thereby precipitating the dramatic morphological changes present in apoptotic cell death [39]. In our present study, we found that TMS and TRAIL synergistically increased the expression of caspases 9, 8, and 3, further

TABLE 3: Effects of TMS + TRAIL on blood cells count *in vivo*.

Treatment	Number of mice	Leukocyte ($\times 10^8$/L)	Erythrocyte ($\times 10^{10}$/L)	Platelet ($\times 10^8$/L)
Control	5	5.17 ± 0.54	7.78 ± 1.04	803.28 ± 84.72
TMS	5	5.02 ± 1.01	7.82 ± 1.03	741.52 ± 107.70
TRAIL	5	4.57 ± 0.63	7.66 ± 0.49	786.76 ± 71.71
TMS + TRAIL	5	4.65 ± 0.72	8.36 ± 0.64	795.46 ± 93.11

No significant changes were detected in the blood cells count among different group of mice ($P > 0.05$).
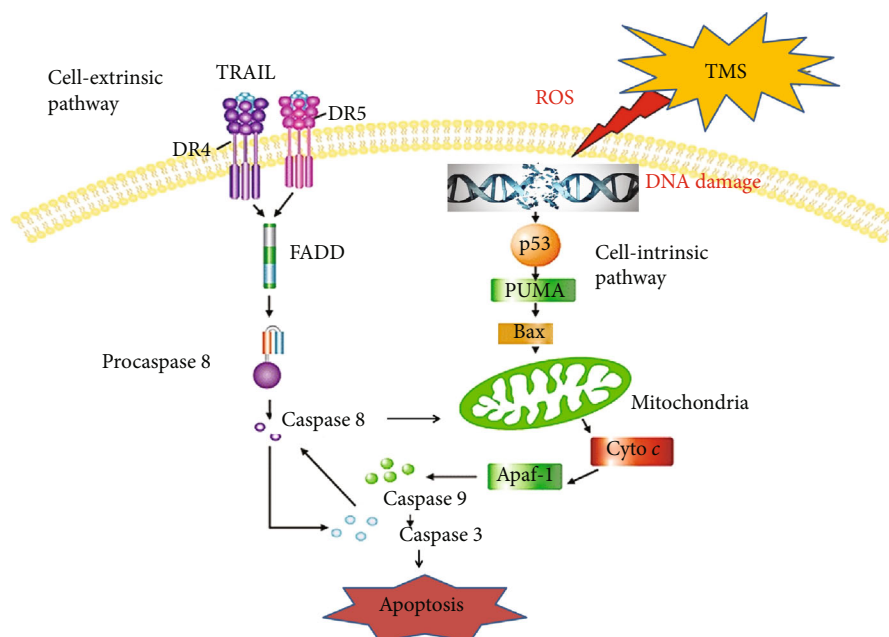

FIGURE 10: Schematic diagram of the mechanisms underlying TRAIL and TMS-mediated apoptosis in osteosarcoma.

highlighting the critical role played by caspases in the apoptosis of osteosarcoma cells. The opening of the mitochondrial permeability transition pore (MPTP), induced by the generation of reactive oxygen species (ROS), is related to the activation of Bax, a pore-destabilizing protein [11]. Our results indicate that increased ROS generation in osteosarcoma cells was detected after treatment with TMS. Furthermore, considerable levels of DNA double-strand breaks were detected in 143B cells after treatment with TMS. Cotreatment using noncytotoxic dosage of TMS and TRAIL led to caspase activation and PARP1 cleavage in 143B cell, which further enhanced ROS-mediated signaling involved in intrinsic apoptosis. However, pretreating cells with the antioxidant (NAC) significantly inhibited intracellular ROS generation and PARP-1 cleavage, thereby reversing apoptosis in osteosarcoma cells induced by cotreatment with TRAIL and TMS. The expression of PUMA and p53 was also decreased by treatment with NAC in 143B cells, which subsequently suppressed apoptosis in these osteosarcoma cells. As a Bcl-2-binding component, PUMA is a proapoptotic protein and can induce p53-dependent apoptosis by transducing a death signal into the mitochondria and activating Bax. Bax is a requisite gateway protein involved in mitochondrial dysfunction and caspase activation [29, 40]. Herein, we found

that combination therapy by TMS and TRAIL remarkably elevated the expression of PUMA and Bax in osteosarcoma cell lines 143B and Saos-2. However, siRNA-induced silencing of *TP53* and *PUMA* expression, or deficiency in the expression of *Bax,* attenuated TRAIL sensitization induced by TMS in osteosarcoma cells. These results indicate that treatment with TMS enhanced intracellular ROS generation, induced DNA damages, and activated the p53/PUMA/Bax signal pathway, resulting in the enhanced outer membrane of mitochondria permeabilization and caspase activation, as well as sensitizing osteosarcoma cell to TRAIL-mediated apoptotic cell death (Figure 10). Despite various novel small molecules and natural compounds have been identified and shown to cause apoptosis by facilitating ROS generation, the specific mechanisms involved in the production of ROS remain unknown [41, 42]. Therefore, in our future studies, we will focus on exploring the mechanisms underlying the biological activity of TMS in the promotion of ROS generation in osteosarcoma cells.

Finally, we explored the potential beneficial effect of cotreatment with TRAIL and TMS in nude mice subjected to orthotopic implantation. Our results demonstrate that cotreatment with TRAIL and TMS suppressed osteosarcoma development with no obvious toxicity in nude mice. The

results of IHC, conducted to assess the expression of PUMA, Bax, and p53 in osteosarcoma tissues collected from the implanted nude mice, further validated the data obtained using our previously described *in vitro* models. In conclusion, our results demonstrate that combined therapy using TRAIL and TMS facilitated intracellular ROS generation, DNA damage, and p53-induced expression of PUMA and Bax in osteosarcoma cells. Activation of p53-PUMA-Bax signaling activated the caspase cascade and induced apoptosis in 143B cells while sparing normal human osteoblasts hFOB1.19. Although our results indicate that TMS may be a safe and effective TRAIL sensitizer and can be used to induce apoptosis in osteosarcoma cells, certain factors require further study. For example, the mechanisms involved in TMS-mediated ROS generation and the efficacy and safety of TMS in patients with osteosarcoma need to be investigated and will be the subject of our future studies.

5. Conclusions

In conclusion, our results indicate that cotreatment with TRAIL and TMS evaluated intracellular ROS level, promoted DNA damage, and activated the Bax/PUMA/p53 pathway, leading to activation of both mitochondrial and caspase-mediated apoptosis in 143B cells.

Abbreviations

TRAIL: TNF-related apoptosis-inducing ligand
TMS: Trans-3, 5, 4$'$-trimethoxystilbene
ROS: Reactive oxygen species
ER: Endoplasmic reticulum
FBS: Fetal bovine serum
DAPI: 4,6-Diamidino-2-phenylindole
PARP-1: Cleaved poly (ADP-ribose) polymerase-1
MAPK: Mitogen-activated protein kinase
DMSO: Dimethyl sulfoxide
MTT: 3-(4,5-dimethylthiazol-2-yl)-2,5-diphenyltetrazolium bromide tetrazolium
PBS: Phosphate-buffered saline
mTOR: Mammalian target of rapamycin
MPTP: Mitochondrial permeability transition pore
DISC: Death-inducing signaling complex.

Data Availability

The primary data used to support the findings of this study are available from the corresponding author upon request.

Conflicts of Interest

The authors declare that there is no conflict of interests regarding the publication of this paper.

Authors' Contributions

M.H. and L.W. conceived the experiments; F.Y.,W.Y., J.L., and J.C. performed the experimental work and acquired and analyzed the data; M.H. wrote the manuscript. L.W. revised the manuscript. All authors reviewed and approved the manuscript.

References

[1] Q. Zhao, J. Zhong, Y. Bi et al., "Gambogenic acid induces Noxa-mediated apoptosis in colorectal cancer through ROS-dependent activation of IRE1α/JNK," *Phytomedicine*, vol. 78, article 153306, 2020.

[2] C. C. Yang, L. D. Hsiao, H. H. Lin et al., "Induction of HO-1 by 5, 8-Dihydroxy-4,7-Dimethoxyflavone via Activation of ROS/p38 MAPK/Nrf2 Attenuates Thrombin-Induced Connective Tissue Growth Factor Expression in Human Cardiac Fibroblasts," *Oxidative Medicine and Cellular Longevity*, vol. 2020, Article ID 1080168, 18 pages, 2020.

[3] M. Hong, J. Li, S. Li, and M. M. Almutairi, "Resveratrol Derivative,Trans-3, 5, 4'-Trimethoxystilbene, prevents the developing of atherosclerotic lesions and attenuates cholesterol accumulation in macrophage foam cells," *Molecular Nutrition & Food Research*, vol. 64, no. 6, article e1901115, 2020.

[4] H. Li, W. K. K. Wu, Z. Zheng et al., "2,3',4,4',5'-Pentamethoxy-trans-stilbene, a resveratrol derivative, is a potent inducer of apoptosis in colon cancer cells via targeting microtubules," *Biochemical Pharmacology*, vol. 78, no. 9, pp. 1224–1232, 2009.

[5] S. E. Aiyar, H. Park, P. B. Aldo et al., "TMS, a chemically modified herbal derivative of resveratrol, induces cell death by targeting Bax," *Breast Cancer Research and Treatment*, vol. 124, no. 1, pp. 265–277, 2010.

[6] F. S. Aldawsari and C. A. Velazquez-Martinez, "3,4',5-trans-Trimethoxystilbene; a natural analogue of resveratrol with enhanced anticancer potency," *Investigational New Drugs*, vol. 33, no. 3, pp. 775–786, 2015.

[7] S. H. Baek, J. H. Ko, H. Lee et al., "Resveratrol inhibits STAT3 signaling pathway through the induction of SOCS-1: role in apoptosis induction and radiosensitization in head and neck tumor cells," *Phytomedicine*, vol. 23, no. 5, pp. 566–577, 2016.

[8] I. Patties, R. D. Kortmann, and A. Glasow, "Inhibitory effects of epigenetic modulators and differentiation inducers on human medulloblastoma cell lines," *Journal of Experimental & Clinical Cancer Research*, vol. 32, no. 1, p. 27, 2013.

[9] M. P. Fuggetta, G. Lanzilli, M. Tricarico et al., "Effect of resveratrol on proliferation and telomerase activity of human colon cancer cells in vitro," *Journal of Experimental & Clinical Cancer Research*, vol. 25, no. 2, pp. 189–193, 2006.

[10] J. A. Giménez-Bastida, M. Á. Ávila-Gálvez, J. C. Espín, and A. González-Sarrías, "Conjugated physiological resveratrol metabolites induce senescence in breast cancer cells: role of p53/p21 and p16/Rb pathways, and ABC transporters," *Molecular Nutrition & Food Research*, vol. 63, no. 22, article e1900629, 2019.

[11] J. Iturri, A. Weber, A. Moreno-Cencerrado et al., "Resveratrol-induced temporal variation in the mechanical properties of MCF-7 breast cancer cells investigated by atomic force microscopy," *International Journal of Molecular Sciences*, vol. 20, no. 13, p. 3275, 2019.

[12] S. Fulda and K. M. Debatin, "Sensitization for tumor necrosis factor-related apoptosis-inducing ligand-induced apoptosis by the chemopreventive agent resveratrol," *Cancer Research*, vol. 64, no. 1, pp. 337–346, 2004.

[13] D. Delmas, C. Rébé, O. Micheau et al., "Redistribution of CD95, DR4 and DR5 in rafts accounts for the synergistic toxicity of resveratrol and death receptor ligands in colon carcinoma cells," *Oncogene*, vol. 23, no. 55, pp. 8979–8986, 2004.

[14] M. Á. Ávila-Gálvez, R. García-Villalba, F. Martínez-Díaz et al., "Metabolic profiling of dietary polyphenols and methylxanthines in normal and malignant mammary tissues from breast cancer patients," *Molecular Nutrition & Food Research*, vol. 63, no. 9, article e1801239, 2019.

[15] F. Möller, O. Zierau, A. Jandausch, R. Rettenberger, M. Kaszkin-Bettag, and G. Vollmer, "Subtype-specific activation of estrogen receptors by a special extract of Rheum rhaponticum (ERr 731), its aglycones and structurally related compounds in U2OS human osteosarcoma cells," *Phytomedicine*, vol. 14, no. 11, pp. 716–726, 2007.

[16] C. Braconi, F. Meng, E. Swenson, L. Khrapenko, N. Huang, and T. Patel, "Candidate therapeutic agents for hepatocellular cancer can be identified from phenotype-associated gene expression signatures," *Cancer*, vol. 115, no. 16, pp. 3738–3748, 2009.

[17] T. Einem Lindeman, M. C. Poirier, and R. L. Divi, "The resveratrol analogue, 2,3',4,5'-tetramethoxystilbene, does not inhibit CYP gene expression, enzyme activity and benzo[a]pyrene-DNA adduct formation in MCF-7 cells exposed to benzo[a]pyrene," *Mutagenesis*, vol. 26, no. 5, pp. 629–635, 2011.

[18] Y. H. Deng, D. Alex, H. Q. Huang et al., "Inhibition of TNF-α-mediated endothelial cell-monocyte cell adhesion and adhesion molecules expression by the resveratrol derivative, trans-3,5,4'-trimethoxystilbene," *Phytotherapy Research*, vol. 25, no. 3, pp. 451–457, 2011.

[19] D. Alex, E. C. Leong, Z. J. Zhang et al., "Resveratrol derivative, trans-3,5,4'-trimethoxystilbene, exerts antiangiogenic and vascular-disrupting effects in zebrafish through the downregulation of VEGFR2 and cell-cycle modulation," *Journal of Cellular Biochemistry*, vol. 109, no. 2, pp. 339–346, 2010.

[20] H. S. Lin and P. C. Ho, "Preclinical pharmacokinetic evaluation of resveratrol trimethyl ether in Sprague-Dawley rats: the impacts of aqueous solubility, dose escalation, food and repeated dosing on oral bioavailability," *Journal of Pharmaceutical Sciences*, vol. 100, no. 10, pp. 4491–4500, 2011.

[21] B. C. Su, C. Y. Pan, and J. Y. Chen, "Antimicrobial peptide TP4 induces ROS-mediated necrosis by triggering mitochondrial dysfunction in wild-type and mutant *p53* glioblastoma cells," *Cancers (Basel)*, vol. 11, no. 2, p. 171, 2019.

[22] S. H. Park, N. M. Phuc, J. Lee et al., "Identification of acetylshikonin as the novel CYP2J2 inhibitor with anti-cancer activity in HepG2 cells," *Phytomedicine*, vol. 24, pp. 134–140, 2017.

[23] M. J. Hsieh, C. W. Wang, J. T. Lin et al., "Celastrol, a plant-derived triterpene, induces cisplatin-resistance nasopharyngeal carcinoma cancer cell apoptosis though ERK1/2 and p38 MAPK signaling pathway," *Phytomedicine*, vol. 58, article 152805, 2019.

[24] U. Weyemi, B. D. Paul, D. Bhattacharya et al., "Histone H2AX promotes neuronal health by controlling mitochondrial homeostasis," *Proceedings of the National Academy of Sciences of the United States of America*, vol. 116, no. 15, pp. 7471–7476, 2019.

[25] E. Moeglin, D. Desplancq, S. Conic et al., "Uniform widespread nuclear phosphorylation of histone H2AX is an indicator of lethal DNA replication stress," *Cancers (Basel)*, vol. 11, no. 3, p. 355, 2019.

[26] E. Saint-Germain, L. Mignacca, G. Huot et al., "Phosphorylation of SOCS1 inhibits the SOCS1-p53 tumor suppressor axis," *Cancer Research*, vol. 79, no. 13, pp. 3306–3319, 2019.

[27] L. Sun, Y. Huang, Y. Liu et al., "Ipatasertib, a novel Akt inhibitor, induces transcription factor FoxO3a and NF-κB directly regulates PUMA-dependent apoptosis," *Cell Death & Disease*, vol. 9, no. 9, p. 911, 2018.

[28] Y. C. Hung, P. W. Wang, T. Y. Lin, P. M. Yang, J. S. You, and T. L. Pan, "Functional redox proteomics reveal that *Salvia miltiorrhiza* aqueous extract alleviates adriamycin-induced cardiomyopathy via inhibiting ROS-dependent apoptosis," *Oxidative Medicine and Cellular Longevity*, vol. 2020, Article ID 5136934, 15 pages, 2020.

[29] J. A. Pulikkan, M. Hegde, H. M. Ahmad et al., "CBFβ-SMMHC inhibition triggers apoptosis by disrupting MYC chromatin dynamics in acute myeloid leukemia," *Cell*, vol. 174, no. 5, p. 1325, 2018.

[30] X. Jiang, S. Fitch, C. Wang et al., "Nanoparticle engineered TRAIL-overexpressing adipose-derived stem cells target and eradicate glioblastoma via intracranial delivery," *Proceedings of the National Academy of Sciences of the United States of America*, vol. 113, no. 48, pp. 13857–13862, 2016.

[31] T. M. Ganten, R. Koschny, T. L. Haas et al., "Proteasome inhibition sensitizes hepatocellular carcinoma cells, but not human hepatocytes, to TRAIL," *Hepatology*, vol. 42, no. 3, pp. 588–597, 2005.

[32] G. Wang, Y. Zhan, H. Wang, and W. Li, "ABT-263 sensitizes TRAIL-resistant hepatocarcinoma cells by downregulating the Bcl-2 family of anti-apoptotic protein," *Cancer Chemotherapy and Pharmacology*, vol. 69, no. 3, pp. 799–805, 2012.

[33] A. Panner, A. T. Parsa, and R. O. Pieper, "Use of APO2L/TRAIL with mTOR inhibitors in the treatment of glioblastoma multiforme," *Expert Review of Anticancer Therapy*, vol. 6, no. 9, pp. 1313–1322, 2006.

[34] L. Kasman, P. Lu, and C. Voelkel-Johnson, "The histone deacetylase inhibitors depsipeptide and MS-275, enhance TRAIL gene therapy of LNCaP prostate cancer cells without adverse effects in normal prostate epithelial cells," *Cancer Gene Therapy*, vol. 14, no. 3, pp. 327–334, 2007.

[35] X. Dai, C. Yin, Y. Zhang et al., "Osthole inhibits triple negative breast cancer cells by suppressing STAT3," *Journal of Experimental & Clinical Cancer Research*, vol. 37, no. 1, p. 322, 2018.

[36] P. Mahalapbutr, P. Wonganan, W. Chavasiri, and T. Rungrotmongkol, "Butoxy Mansonone G inhibits STAT3 and Akt signaling pathways in non-small cell lung cancers: combined experimental and theoretical investigations," *Cancers (Basel)*, vol. 11, no. 4, p. 437, 2019.

[37] N. Chhiber, T. Kaur, and S. Singla, "Rottlerin, a polyphenolic compound from the fruits of Mallotus phillipensis (Lam.) Mull.Arg., impedes oxalate/calcium oxalate induced pathways of oxidative stress in male wistar rats," *Phytomedicine*, vol. 23, no. 10, pp. 989–997, 2016.

[38] D. I. Radke, Q. Ling, R. Häsler, G. Alp, H. Ungefroren, and A. Trauzold, "Downregulation of TRAIL-receptor 1 increases TGFβ type II receptor expression and TGFβ signalling via microRNA-370-3p in pancreatic cancer cells," *Cancers (Basel)*, vol. 10, no. 11, p. 399, 2018.

[39] D. P. Denning, V. Hatch, and H. R. Horvitz, "Programmed elimination of cells by caspase-independent cell extrusion in C. elegans," *Nature*, vol. 488, no. 7410, pp. 226–230, 2012.

[40] A. B. Hua, R. Justiniano, J. Perer et al., "Repurposing the electron transfer reactant phenazine methosulfate (PMS) for the apoptotic elimination of malignant melanoma cells through induction of lethal oxidative and mitochondriotoxic stress," *Cancers (Basel)*, vol. 11, no. 5, p. 590, 2019.

[41] X. Liu, P. Zhao, X. Wang et al., "Celastrol mediates autophagy and apoptosis via the ROS/JNK and Akt/mTOR signaling pathways in glioma cells," *Journal of Experimental & Clinical Cancer Research*, vol. 38, no. 1, p. 184, 2019.

[42] Y. Zhou, L. Wei, H. Zhang et al., "FV-429 induced apoptosis through ROS-mediated ERK2 nuclear translocation and p53 activation in gastric cancer cells," *Journal of Cellular Biochemistry*, vol. 116, no. 8, pp. 1624–1637, 2015.